Nitric oxide-dependent bone marrow progenitor mobilization by carbon monoxide enhances endothelial repair after vascular injury

Published in final edited form as:
Circulation. 2010 February 2; 121(4): 537–548. doi:10.1161/CIRCULATIONAHA.109.887695.

Nitric Oxide-Dependent Bone Marrow Progenitor Mobilization by Carbon Monoxide Enhances Endothelial Repair Following Vascular Injury

Barbara Wegiel, PhD[#,‡], **David J. Gallo, B.S.**[=], **Kathleen G. Raman, MD**[*,#], **Jenny M. Karlsson, M.S.**[§], **Brett Ozanich, B.S.**[*], **Beek Y. Chin, PhD**[‡], **Edith Tzeng, MD**[*], **Shakil Ahmad, PhD**[¶], **Asif Ahmed, PhD**[¶], **Catherine J. Baty, PhD**[§], and **Leo E. Otterbein, PhD**[‡]

[‡] Transplantation Institute, Department of Surgery, Beth Israel Deaconess Medical Center, Harvard Medical School, Boston, MA, USA

[*] Department of Surgery, University of Pittsburgh School of Medicine, Pittsburgh, PA, USA

[§] Department of Cell Biology and Physiology, University of Pittsburgh School of Medicine, Pittsburgh, PA, USA

[=] Alfama Inc., Lisbon Portugal

[¶] Department of Reproductive and Vascular Biology, Institute for Biomedical Research, University of Birmingham, Birmingham, UK

Abstract

Background—Carbon monoxide (CO) has emerged as a vascular homeostatic molecule that prevents balloon-angioplasty-induced stenosis via anti-proliferative effects on vascular smooth muscle cells (VSMC). The effects of CO on re-endothelialization have not been evaluated.

Methods and Results—Exposure to CO has diametrically opposite effects on EC and VSMC proliferation in rodent models of carotid injury. In contrast to blocking VSMC growth, CO

Correspondence should be addressed to: Leo E. Otterbein, PhD, Associate Professor of Surgery, Harvard Medical School, Transplant Institute, Beth Israel Deaconess Medical Center, Center for Life Sciences, 3 Blackfan Circle; Rm 603, Tel: 617-735-2851, Fax: 617-735-2851, lotterbe@bidmc.harvard.edu.
[#]denotes equal contribution

Clinical summary

Carbon monoxide is now recognized as a potent therapeutic molecule at low, nontoxic doses. CO is currently in Phase II Clinical Trials to improve kidney function after transplant of a kidney allograft. Inhaled CO is known to block intimal hyperplasia following balloon angioplasty. The data presented here offer continued insight into a potential therapeutic adjuvant involving treatment with CO gas or local delivery with a CORM to substitute or compliment stent placement and prevent intimal hyperplasia. We demonstrate that CO prevents intimal expansion in mice in part by early and enhanced reendothelialization of the injured vessel. CO enhances proliferation, recruitment and migration of neighboring endothelial cells (EC) as well as potent recruitment of bone marrow-derived progenitor cells to the site of injury. Accelerated reendothelialization adds to the clinical vascular cytoprotective benefits achieved with short exposures to CO. This observation describing the effects of CO on EC proliferation is in direct contrast to vascular smooth muscle cells (VSMC), the proliferation of which is blocked by CO. Mechanistically, CO via distinct non-overlapping signal transduction pathways in EC versus VSMC. Nitric oxide regulates EC function while guanylate cyclase regulates VSMC function. Our studies demonstrate that CO is a vasoprotective gas that acts via multiple mechanisms to best re-establish vessel homeostasis. Collectively, our data support the use of CO as a therapeutic modality in the treatment of vascular proliferative disorders.

Disclosures

We declare that there are no conflicts of interest and nothing to disclose.

administered as a gas or as a CO releasing molecule (CORM) enhances proliferation and motility of EC *in vitro* greater then 50% vs air controls, and *in vivo* accelerates re-endothelialization of the denuded artery by day 4 after injury versus day 6 in air-treated animals. CO enhanced EC proliferation via rapid activation of RhoA followed by downstream phosphorylation of Akt, eNOS phosphorylation and a 60% increase in NO generation by the EC. CO drives cell cycle progression through phosphorylation of retinoblastoma (Rb), which is in part dependent on eNOS-generated nitric oxide (NO). Similarly, endothelial repair *in vivo* requires NO-dependent mobilization of bone marrow-derived EC progenitors (EPC) where CO showed a 4-fold increase in the number of mobilized GFP-Tie-2 positive EPC versus control with a corresponding accelerated deposition of differentiated GFP-Tie-2 positive EC at the site of injury. CO was ineffective in augmenting EC repair and the ensuing development of intimal hyperplasia in *enos*$^{-/-}$ mice.

Conclusions—Collectively our data demonstrate that CO accelerates EC proliferation and vessel repair dependent on NO generation and enhanced recruitment of bone marrow-derived endothelial progenitor cells.

Keywords

balloon; endothelium; nitric oxide synthase; signal transduction; stenosis

Introduction

Proliferation of VSMC and their acquisition of a pro-inflammatory phenotype are central events in the pathogenesis of vascular lesions including vein occlusion, post-angioplasty restenosis and transplant arteriosclerosis[1–3]. Restenosis rates at one year approach 30% without stents versus 5% in patients that receive stents. Greater then 95% of percutaneous coronary interventions involve stenting[4, 5,6]. While the stents hold great promise, there continues to be a need for advances in current therapies. Drug eluting stents are now used as novel drug delivery devices including Rapamycin/Sirolimus coated devices to further reduce stenosis by interfering with VSMC proliferation[7, 8]. Drug eluting stents however are complicated by in-stent thrombosis resulting from delayed endothelialization if anti-platelet therapies are stopped. Appropriate re-endothelialization of a stent or denuded vessel becomes crucial for effective vascular homeostasis. In this study, we hypothesized that CO administered as an inhaled gas or via a CO-releasing molecule would provide vascular protection by facilitating EC repair and prevent intimal hyperplasia. We demonstrated previously that a 1 hr exposure to CO at low, non-toxic concentrations before injury with no further treatment prevents the development of intimal hyperplasia caused by balloon angioplasty via direct effects on VSMC proliferation[9]. Growth arrest in these cells occurred via a pathway sequentially involving cGMP, p38 MAP kinase and p21. Interference at any point in this cascade resulted in abrogation of the CO effects. CO, like nitric oxide (NO) is very pleiotropic in its effects, modulating cellular behavior and physiology in diverse ways depending on the cell type, circumstance and model being evaluated[10, 11]. The end result, however, is that CO functions to re-establish vascular stability.

We hypothesized that the endothelium and more specifically the endothelial cells that are physically injured through denudation trauma during the balloon procedure are also a target by which CO would exert beneficial effects. Heme oxygenase-1 (HO-1), the cytoprotective enzyme responsible for the generation of endogenous CO, was shown to regulate EC proliferation *in vitro*[12], however the role and the mechanism of action of HO-1 and CO in EC repair following trauma has not been evaluated. HO-1-deficient mice show an exaggerated response to vessel injury. We reasoned that CO, in addition to an anti-apoptotic role in EC[13], would enhance proliferation and migration of EC and promote vessel repair by facilitating mobilization of endothelial progenitor cells (EPC). The knowledge that NO promotes survival,

proliferation of EC and EPC mobilization[14–16], prompted us to investigate the hypothesis that endothelial nitric oxide synthase (eNOS) may play a role in the CO effects on EC.

In this study we describe the effects of CO as well as a CORM on the augmentation of EC proliferation, migration and EC progenitor mobilization to the injured site in well-established rodent models of vascular trauma[3]. We show that CO accelerates re-endothelialization of the injured vessel and identify eNOS and NO as essential for the CO effect. In EC, activation of Akt, eNOS and retinoblastoma (Rb) protein dominate to accelerate cell cycle progression and EC migration. The diametrically opposite effects of CO on proliferation of EC and VSMC are clear evidence of the pleiotropic homeostatic effects of CO, in this case preventing development of the intimal lesion by acting through disparate modes of action on these two vascular cell types.

Materials and Methods

Cell culture and pharmacologic reagents

Rat primary aortic endothelial cells (RAEC) were purchased from VEC Technologies (Rensselaer, NY) and were maintained in the MCDB-131 Complete medium with antibiotics and growth factors (VEC Technologies, NY) on 0.2% gelatin coated plates. Cells were used between passages 3–10. Bone marrow derived endothelial progenitor cells from Tie-2-GFP mice (Tie2 receptor is expressed in endothelial linage cells [17]) were cultured in EBM-2 medium as described[18]. Cells were exposed to 250 ppm CO, 5% CO_2 in 95% N_2 as previously described[19]. CORM (ALF421/CORMA-1, Alfama Inc.) was used at a concentration of 1–20 μM unless otherwise stated. We employed iCORM (inactive) as a negative control where indicated. VSMC were isolated from mouse aortas and grown in DMEM containing 15% FBS. Pharmacologics used include: the selective inhibitor of nitric oxide synthase, N(G)-nitro-L-arginine methyl ester (L-NAME, 100 μM from Sigma), the PI3K inhibitor, LY294002 (10mM, Sigma) was used at 10 μM. RAEC cells were pretreated for 1 hr with inhibitors followed by CO or Air treatment.

Adenoviral transduction—Adeno-dominant negative mutant RhoA and constitutively active RhoA were kindly gifted by Dr. James Bamburg as previously described [20]. Y5 and GFP-adenoviruses were used as controls. All viruses were used at 10 MOI for infection of RAEC. Adenoviruses were prepared in serum free medium and added for 6 hr to the cells. Cells were then washed with PBS and fresh serum-containing medium was added to the cells and incubated for 48 hr prior to use.

Plasmids and transfections—Dominant-negative mutant (DNM) Akt and control constructs were kindly gifted by Dr. Alex Toker (BIDMC, Boston). For transfection experiments, RAEC cells were transfected with Superfect Reagent (Qiagen) according to the vendor's protocol. Transfection efficiency was evaluated by GFP and was determined to be on average 40–50%.

Proliferation assays

The effect of CO on proliferation of RAEC cells was determined using the non-radioactive BrdU based cell proliferation assay (per manufacturers guidelines (Roche)).

Thymidine incorporation was measured in growth-arrested VSMC and EC stimulated to proliferate with 10% FBS in the presence of 5μCi/mL of ^{3}H-thymidine (NEN, Boston, MA) for 24 hr ± CO as indicated.

Cell motility and migration

Described in supplementary methods section.

Cell cycle studies

RAEC cells were starved for 20 h in serum-free medium. Serum containing medium was then applied together with pharmacologics ± CO for 6–24 h. After harvesting, cells were fixed and permeabilized with 70% ice-cold ethanol for 30 min, washed twice with 1x PBS, resuspended and incubated in FACS buffer containing 5 mg/ml propidium iodide (Sigma), 100 mM sodium citrate, pH 7.3 and 0.05 mg RNase A (Sigma) for 30 min at 4 °C. Cell fluorescence was measured by FACS.

RhoA activation

Activity of the small GTPase, RhoA was determined by use of EZ-Detect™ Rho Activation Kit (Pierce, US) according to the manufacturer's protocol.

Immunoblotting and Phalloidin

Described in supplemental methods section.

NO generation

Fluorescence—RAEC were loaded with the NO selective flourophore 4-amino-5methylamino-2′,7′-difluorescein diacetate (DAF-FM; Molecular Probes, Carlsbad CA) 20 min prior to exposure to air or CO (250ppm) for 5–60 min. Cells were fixed and fluorescence assed by flow cytometry with an excitation/emission of 495/515nm at various time points.

Chemiluminescence—HUVEC were plated onto 24 well plates and treated for 1 hour in the presence and absence of CO gas (250 ppm) and NO was measured in cell supernatants using a Sievers chemiluminescent NO analyzer as described [21].

Carotid artery injury model in rats and mice

Male Sprague Dawley rats (250–300g) were purchased from Harlan Laboratories and mice from Jackson Laboratories. Balloon angioplasty and wire injury was carried out as described previously.[11] Injury of the vessel wall and subsequent pathological analysis was made in a manner that was blinded to the treatment group and performed by trained scientists. Male C57BL/6, and *enos*$^{-/-}$ mice (7–8 weeks) and Tie2-GFP mice were purchased from Jackson Laboratories (Bar Harbor, Maine). Mice were treated with CO (250 ppm for 1 hr) or ALF 421 (10 mg/kg, i.p. 1 hr before and 1 hr after) or iCORM). Water or air was used as controls. All animals were housed in accordance with the American Association for Laboratory Animal Care. The carotid injury and bone marrow transplantation protocols were approved by Beth Israel Deaconess Medical Center's Institutional Animal Care and Use Committee.

Immunostaining and cell population histomorphometric analysis

Vessels were harvested 1, 3 and 5 days after angioplasty. Rat leukocyte and endothelial cell populations were detected using anti-rat macrophage (CD68, ED-1), ICAM-1 (CD54; 1A29), myeloperoxidase and CD31. Mouse vessels were stained for H&E and Sca1+ and CD31 as previously described [22]. Eight to ten images were captured from each injured carotid and analyzed as detailed above. I/M ratio was measured as previously described[9]. RAEC were seeded on microscopic slides and treated with or without CO for 24 hr. Cells staining with P-Histone H3 antibodies was applied as previously described [22].

Bone marrow transplantation and generation of Tie-2 GFP chimeras

Wild-type C57BL/6J mice were lethally irradiated (12 Gy). On the same day, mice were injected with 5×10^6 bone marrow cells from Tie-2-GFP mice (as above). Reconstitution of bone marrow was determined by flow cytometry 1 month after transplantation. Tie-2 GFP chimeras were used for the experiments as described above. The average percent reconstitution was determined to be between 90–95% with 0.9–12% Tie-2-GFP-positive cells in the marrow 4–6 weeks after transplantation.

Colony outgrowth assay

Colony outgrowth assay was performed as previously described[23]. C57B6 mice were exposed to CO (250ppm) or Air for 1 hour and blood samples were collected. Mononuclear cells were freshly isolated using Ficoll gradient (20 min, 500 × g) and seeded on the 0.2% gelatin-coated plates in EGM Endothelial growth medium supplemented with EGM Bullet Kit (Clonetics Lonza, San Diego). Colonies were counted and photographed 10 days after isolation of mononuclear cells.

Flow Cytometry

To assess the percentage of GFP-positive endothelial cells, which were mobilized to the circulation after CO/air treatment, blood samples were harvested from animals 12 hours post-wire injury. Red blood cells were lysed at RT for 5min with erythrocyte lysis buffer, following by washing with PBS. Cells were fixed with 2% PFA and blocked with 1% BSA in PBS followed by staining with antibody against GFP (Invitrogen, CA) for 1 hour at RT. Secondary antibody conjugated with fluorescein were applied for 1 hour at RT. Cells were analyzed on a FACScan flow cytometer (Becton Dickinson). The chimeric mice were housed in the BIDMC facility according to IACUC approved protocols. The average percent reconstitution was determined to be 0.9–1.2% GFP-Tie2 positive cells in the marrow 4–6 weeks after transplantation.

Statistical Analyses

In all in vitro the experiments, the significance of difference was determined using one or two-way ANOVA (with post-hoc Tukey test) as described in the figure legends (SPSS Inc, Chicago, IL). Non-parametric Wilcoxon test was used where indicated. Statistical analyses was applied to all independent experiments with significance accepted at $p<0.05$.

Results

CO augments EC proliferation

To test the effects of CO on EC proliferation, primary rat aortic endothelial cells (RAEC) were exposed to CO (250 ppm) and [^{3}H]thymidine or BrdU incorporation was evaluated 24 h later. CO gas significantly increased EC proliferation over air-treated cells as assessed by DNA synthesis (Figure 1A–B). Similarly, a CORM, in a concentration-dependent manner, induced significant proliferation of RAEC (Supplementary Figure 1A). FACS analyses by PI staining showed that cells exposed to CO had a greater accumulation in S phase versus air-treated cells (Figure 1C). Importantly, the effect of CO or CORM was unlikely to be due to hypoxia as exposure of RAEC cells to hypoxia (1% O_2), inhibited proliferation of RAEC (Supplementary Figure 1B). To corroborate the CO effects on cell cycle we evaluated cells for phosphorylated histone H3 and retinoblastoma (Rb) expression by immunostaining and immunoblotting respectively (Figure 1D–E, Supplementary Fig 2A) and observed increased phosphorylation of both proteins. Treatment with CORM also induced significant phosphorylation of Rb at 24 hours versus vehicle control (Figure 1F). These results in EC contrast directly with the effects of CO on VSMC proliferation, which when exposed to identical conditions, showed significant

growth arrest ($8.5\pm0.1\times10^6$ cpm/well in air treated versus 3.85 ± 0.09^6 cpm/well in CO treated cells ($p<0.01$) as reported previously[9] but presented here again for comparison[9, 24, 25].

CO increases EC motility

Employing live cell time-lapse microscopy, we next evaluated the effects of CO exposure on EC motility. Using the well-described 'scratch' model, we disrupted an endothelial monolayer simulating EC denudation, to mimic that which occurs during angioplasty trauma, and exposed the cells to media saturated with air or 250 ppm CO. In those cells exposed to CO, we observed a 2-fold greater motility rate versus air controls (Figure 2A). These data demonstrate that CO not only increased proliferation of EC (Figure 1) but also their motility. Immunostaining for F-actin showed that EC exposed to CO show a greater propensity for cytoskeletal organization correlating with motility measurements (Figure 2B–C; Air versus Figure 2D–E; CO). CO-treated cells show a highly organized actin distribution with stress fibers forming dense peripheral and polarized bands at the leading edge, which is otherwise irregular and punctate in air-treated cells.

CO activates RhoA and Akt kinase in EC, which regulates CO-induced proliferation

We next attempted to elucidate the signaling mechanisms that were influenced by CO to control EC proliferation. Due to the high diffusivity of CO, we hypothesized that CO would elicit a rapid effect on the cell initiated at the cell membrane. We assessed expression of the small GTPase RhoA, which is important in cell growth, cytoskeletal organization and an initiator of downstream signaling events. Exposure of EC to CO resulted in a strong and rapid time-dependent activation of RhoA (Figure 3A). Downstream of RhoA are the MAP kinases as well as Akt[26] both of which have been shown to be modulated by CO[27, 28]. We first evaluated p38 activation, which was modestly decreased (data not shown) and thereby in direct contrast to effects of CO observed in VSMC[29]. Akt has been shown by others to be activated by CO, albeit in an inconsistent fashion depending on the cellular model. One report demonstrated in human endothelial cells that CO inhibits Akt activation[30] while another report showed that CO increases Akt in heart tissue from rats undergoing ischemia/reperfusion injury[28]. We therefore wanted to assess the effects in our model. In RAEC exposed to CO, we observed a time-dependent induction of Akt phosphorylation (Figure 3B, Supplementary Figure 2B). Treatment of RAEC with CORM induced similar levels of phosphorylated Akt, confirming that observed with gaseous CO (Figure 3C). The effect of CO on Akt activation was abrogated in the presence of RhoA-DNM (data not shown). Employing a selective and well-characterized pharmacologic inhibitor of PI3K (LY290024), we evaluated the role of PI3K-dependent Akt on CO-induced proliferation of EC. Blockade of PI3K led to a partial inhibition of the effects of CO on phosphorylation of Rb (Figure 3D) and EC proliferation (Figure 3E). To strengthen our observation that Akt was linked to enhanced EC proliferation by CO, we transiently transfected RAEC with a dominant negative mutant Akt expression vector (Figure 3F). Employing both pharmacologic and genetic methodologies to block Akt, the effects of CO on augmenting proliferation was lost in cells without functional Akt signaling (Figure 3D–F) vs control. Finally, we examined the role of RhoA on CO-induced proliferation and observed a partial reversal of the CO effects in RAEC cells transduced with a RhoA-DNM (Figure 3G).

CO increases expression of eNOS and NO generation in RAEC

We have shown in previous work that there is an interrelationship between the gases CO and NO, particularly in the vasculature[31, 32,33]. We hypothesized that one mechanism by which CO induces enhanced proliferation following injury involved effects on eNOS activation and NO generation given the relatively high expression of eNOS in EC. RAEC exposed to CO gas or a CORM showed a time-dependent increase in phosphorylation of eNOS and NO generation in EC as measured by immunoblotting, DAF fluorescence and chemiluminescence (Figure

4A–E). Interestingly, CO gas showed slightly slower kinetics compared to the CORM, which we speculate might be due to the kinetics of gas exposure versus direct delivery of a CO releaser into the culture media. To validate the importance of this activation, we administered the selective NOS inhibitor L-NAME and evaluated proliferation by BrdU incorporation as well as phosphorylation of Rb. In the presence of NO blockade, CO was unable to impart pro-proliferative effects, returning growth patterns to that of air controls (Figure 4F) and preventing increases in phospho-Akt and –Rb (data not shown). These data support the interrelationship of these gases *in vitro* in regulating proliferation of RAEC and suggest that CO not only increases eNOS phosphorylation, but also influences its activity to generate NO and importantly drive activation of Akt and Rb. The relationship between NO, Akt and Rb in EC has been described in the literature in other models, but to date has not been evaluated with CO in EC[34, 35]. We describe here that CO clearly triggers activation of this pathway. NO has been shown to impart pro-survival effects in EC[14, 36]. We conclude that by imparting pro-survival benefits to the EC, NO is critical in allowing CO to act via a RhoA→ Akt → Rb cascade to augment proliferation.

CO augments re-endothelialization following balloon angioplasty in rats and wire trauma in mice

CO can limit vascular occlusion, driven primarily by reduced intimal thickening over the course of weeks. To date, the effects of CO treatment on early events that occur following injury within the first 3–5 days has not been evaluated. We exposed rats to either air or CO for 1 hr prior to angioplasty as described previously and evaluated the effects on re-endothelialization following balloon trauma. Importantly, the animals were not exposed to CO again. We harvested vessels at 1, 3 and 5 days post injury and stained sections for CD31 and ICAM; markers specific for EC, which are readily observed in uninjured vessels (Figure 5A). In animals exposed to air, the EC monolayer was absent at 1, 3 and 5 days (Figure 5B) post angioplasty, but fully restored by 7 days. In contrast, animals exposed to 1 hr of CO showed a complete restoration of the EC monolayer by 5 days (Figure 5C) (5/6 animals in CO versus 0/6 animals in Air, $p<0.03$). In these same vessels, we evaluated the inflammatory response and observed increased macrophages (Supplementary Figure 3A) and neutrophils (data not shown) infiltrating the lesion at day 3–5 post angioplasty, which were both inhibited by CO. *In vitro*, both CO and CORM treatment effectively inhibited trans-membrane migration of U937 monocytes (Supplementary Figure 3B–C). We also evaluated the effects of CO on EC restoration in the murine model of wire trauma, a well-accepted surrogate for angioplasty. As was observed in rats, CO also enhanced repair of the endothelium in mice restoring the EC monolayer by day 4 (Figure 6A) while air-controls showed little to no EC presence until days 5 and 6 post injury (data not shown). We also demonstrate that administration of CORM ALF-421, prior to and just after wire injury, also accelerated re-endothelialization in the carotid similar to CO gas (Figure 6B). The COHb levels achieved with CORM was 11±2% versus 15 ±3% with 250 ppm for 1 hr. A separate cohort of mice were also treated with inactive CORM (iCORM), which failed to enhance EC repair following injury (Figure 6B).

CO requires NO to enhance re-endothelialization

Our *in vitro* studies showing that CO increased NO generation in part through phosphorylation of eNOS, prompted us to evaluate whether CO would enhance repair in the absence of eNOS *in vivo*. CO was unable to enhance re-endothelialization in *enos*$^{-/-}$ mice at 4 days versus CO-exposed wt mice (Figure 6C). To begin to assess a link between re-endothelialization and development of intimal hyperplasia, we also evaluated the ability of CO to block the development of intimal hyperplasia in *enos*$^{-/-}$ versus wt mice in the presence of CO having demonstrated previously that CO can inhibit intimal hyperplasia in response to wire trauma[9]. We validated that again here and additionally demonstrate that CO was unable to prevent intimal hyperplasia in the absence of NO (Figure 6D–E). We observed similar effects in rats

where NO was blocked by administering L-NAME ± CO (data not shown). While this could be interpreted as NO being also absent in VSMC in these animals, we showed previously that neither eNOS nor iNOS were important in the ability of CO to inhibit growth of VSMC[9].

CO increases progenitor cell recruitment into the circulation and the injured vessel

Re-endothelialization of injured vessels is thought to be in part, driven by the influx of undifferentiated progenitor cells. We therefore tested the hypothesis that CO-targeted and enhanced progenitor cell influx into the denuded site following injury via the expansion of the bone marrow pool of EC and mobilization of endothelial progenitor cells (EPC). Immunostaining of vessels from wire-injured mice showed that CO exposed animals had a significantly higher number of $sca1^+$ cells at the site of injury vs air-treated controls (Supplementary Figure 4). Interestingly, the $sca1^+$ cells did not express CD34 at this time point and we speculate that this phenotypic change occurs rapidly particularly with CO and likely in the adventitia. We speculate that the enhanced recruitment is in part responsible for the more rapid infiltration and repair. Assessment of outgrowth colonies showed that CO enhanced the number of colonies by 6–8 fold vs control mice ($p<0.001$). We next exposed progenitor cells to CO in culture and observed that CO induced differentiation of progenitors into EPC/EC. Bone marrow progenitor cells purified from Tie-2-GFP mice, were exposed to CO for 3 days in culture. In these cells, Tie-2, which is a specific EC promoter is linked to GFP therefore GFP can be used as a surrogate marker for mature EC (Figure 7A). Air treated cells showed limited expression of GFP by day 3, in contrast to CO treated progenitors which showed a 2–3 fold increase in GFP expression vs air treated (Figure 7B–D). As a control for specificity of EC proliferation, we also differentiated progenitors into macrophages by treating with M-CSF and saw no effects of CO on GFP after differentiation (Figure 7B). These data thus support a direct effect of CO in inducing progenitor cells to differentiate into EC. To recapitulate *in vivo* our observations *in vitro*, we generated Tie-2 GFP chimeric mice and analyzed EPC mobilization into the blood after wire injury at 12 hours (Figure 8A–B). We selected this time point as we observed a strong recruitment of $sca\text{-}1^+$ positive cells to the injured vessel after CO exposure at 12 hours (Supplementary Figure 4). Vessel injury alone induced recruitment of ~5% GFP-positive EPC to the circulation (Figure 8A–B). Pre-treatment with CO however, before vessel injury, induced a further 2–5 fold enhancement of GFP-positive endothelial progenitor cell mobilization into the blood (Figure 8A–B). Enhanced mobilization of BM-derived progenitors after CO exposure for 1h was further confirmed by performing a colony outgrowth assay. Blood mononuclear cells were collected from mice exposed to air or CO and then cultured in EC media for 10 days after isolation. CO significantly increased colony numbers over air-treated and in some of the wells, we observed tubule formation in response to CO (Supplementary Figure 5). Finally, we assessed whether GFP-positive EPC in the Tie-2-GFP chimeric mice contribute to re-endothelialization of the vessel following CO treatment. We detected GFP-positive endothelial cells in the injured vessels following CO treatment at day 4 (Figure 8C–D). We detected no GFP-positive cells in air treated mice as EC repair was not present at day 4 (Figure 8C–D). Collectively these data suggest that CO-enhanced EC repair occurs in part via enhanced mobilization and differentiation of EPC.

Discussion

The denudation of the endothelium caused by physical balloon trauma, combined with a rapid increase in leukocyte infiltration leads to increased smooth muscle cell proliferation and formation of the neointima. The loss of the endothelium is perhaps the initiating element associated with subsequent vaso-occlusion. The direct effects of CO to induce growth arrest of VSMC and prevent intimal expansion in vivo are clear, driven primarily by a c-GMP-p38-p21 signaling pathway that is NO-independent[9,32]. We hypothesized that CO must initiate additional mechanisms involved in repair of the vessel that contribute to inhibition in the

intimal expansion following trauma. Namely, CO would modulate the acute inflammatory response, i.e. leukocyte infiltration, as well as targeting the endothelium to facilitate in the regeneration/replacement of this barrier lamina. We employed both the clinically relevant balloon injury model in rats and the wire injury trauma model in mice that permitted mechanistic experiments to test the effects of CO on the early events following vessel trauma.

The effects of CO in restoring homeostasis continue to implicate a critical role for NO. NO is a potent pro-survival factor in EC, unlike VSMC.[37,38] We thus hypothesized that NOSIII/eNOS would be a likely target for CO in EC to increase NO through direct binding to NOS or via specific signal transduction and contribute to survival even if NO did not necessarily promote a proliferative response. Increased survival would then allow other signaling pathways, such as phosphorylation of Rb, to promote growth. Our data suggests that one mechanism by which CO promotes cell growth is through phosphorylation of eNOS and activation of Akt and Rb. The ability of CO to increases eNOS phosphorylation however may occur indirectly though an upstream potassium channel-mediated event that leads to activation of PI3K and Akt. Blockade of potassium channels resulted in a loss of the effects of CO on EC proliferation (unpublished observation) and CO is known to function in part through activation of this channel.[39]

Cyclins and CDKs induce hyperphosphorylation of Rb, liberating E2F and other transcription factors such as YY1, which play a pivotal role in the coordinated transactivation of cell cycle regulatory genes.[24] It is a formal possibility that CO modulates growth and genome transcription at the level of histone and chromatin modification. CO-induced mitosis is blocked by the inhibitor of histone deacetylase, trichostatin (unpublished observation). Our results clearly demonstrate that exposure to CO in EC leads to quick activation of the small G-protein RhoA, accelerated entrance into S-phase with increased phosphorylation of Rb that results in enhanced growth. We however cannot exclude the possibility that CO activates other molecules involved in cytoskeletal organization and signaling. CO promotes migration of the EC in the scratch assay. The exact mechanism by which CO modulates the cytoskeleton remains to be fully elucidated likely involves in part the RhoA signaling machinery described herein that is known to be involved in the F-actin cytoskeleton re-organization and stress fiber formation. Combining our observations *in vitro* and *in vivo* including bone marrow progenitor cell recruitment to the site of injury supports the concept that CO administered as a gas or CORM fosters earlier re-endothelialization and involves recruitment, differentiation and motility of EC in an effort to augment repair of the injured vessel ultimately contributing to less intimal hyperplasia. The CO-mediated benefit is sustained for more than 21 days despite the one-time exposure of the animals to CO, indicating that the process of vascular remodeling is in large measure determined very early following acute injury. The kinetics of the events leading to augmentation of repair are multi-factorial and clearly reflect decreased inflammation, earlier EC deposition and ultimately decreased hyperproliferation of VSMC. In a model of pulmonary hypertension in rodents, we demonstrated that intermittent exposure to CO, initiated after the establishment of disease, results in reverse remodeling, i.e. back to original architecture and function.[32] In these animals, CO induced EC to generate NO that ultimately led to restoration of normal artery and vessel size. In this instance CO-induced NO arose from the EC present in the vessels. In the data presented here where EC are not present at the time of CO exposure, the origin of the EC is likely circulating or recruited endothelial progenitors based on our GFP data, or a significant contribution from the EC immediately adjacent to the denuded lesion that proliferate and mobilize into the injured area perhaps driven by an augmented chemokine gradient elicited by NO such as SDF. SDF has been demonstrated to be involved in the ability of HO-1 to regulate angiogenesis.[40] HO-1 deficient mice were unable to form capillary sprouts, which was reversed by administration of a CO releasing molecule. The mechanism by which HO-1/CO regulates angiogenesis is different then what we describe here and involves VASP and PGE2 versus the Akt-eNOS-Rb pathway.[12, 40] Perhaps this speaks to the vast differences

between the processes of neovascularization and EC repair. In this same vein, eNOS/NOSIII is essential for EPC mobilization[41]. Neovascularization does not occur in mice lacking eNOS, strongly supporting the observations described here that CO requires NO to enhance re-endothelialization of denuded vessels.

From a therapeutic standpoint, these results combined with our data that CO prevents neointima formation following trauma, combine three actions: i.) anti-inflammatory effects, ii.) direct effects on VSMC to block proliferation and iii.) pro-proliferative actions on EC that lead to rapid re-endothelialization of the denuded EC lesion. As such, exposure to CO results in greater efficacy in preventing neointima formation and stenosis following balloon angioplasty versus other approaches aimed at the sole blockade of VSMC proliferation[42–44]. One of the principal challenges with stent therapy is the inability of the stent to become endothelialized as the coatings also limit EC proliferation. The data presented here offer a potential therapeutic adjuvant involving treatment with CO gas or local delivery of a CORM to substitute or compliment stent placement perhaps even impregnating one of the emerging CORM molecules onto a stent. Either mode of CO delivery would in principal yield the same beneficial result. If the pulmonary data holds true showing that exposure to CO can reverse intimal expansion without intervention, the need for angioplasty and stents might be reduced, which would be particularly useful in the peripheral circulation where drug eluting stents have not proven as efficacious, with restenosis rates approaching 30% at one year.

In conclusion, we demonstrate a novel function of CO in promoting re-endothelialization that likely is the result of enhanced proliferation, recruitment and migration of neighboring EC. Additional experiments are currently underway to address the detailed mechanism as well as whether chronic delivery of CO would be needed to prevent long term restenosis and reduce the need for reintervention. Of course with longer term CO exposure careful safety data will be necessary. Accelerated re-endothelialization adds to the clinical vascular protective benefit achieved by short exposures to CO prior to angioplasty. The sooner re-endothelialization has occurred in the vessel, the sooner the entry of circulating monocytes and T cells will be blocked, thereby limiting inflammation and subsequent vasoocclusion [45]. Finally, these data identify, delineate and add to the growing database of the interrelationship between the two gas molecules NO and CO in vascular-proliferative diseases that in tandem act to re-establish homeostasis. With careful clinical testing, CO may prove to be a novel therapeutic in the treatment of numerous vascular disease syndromes.

Supplementary Material

Refer to Web version on PubMed Central for supplementary material.

Acknowledgments

Funding Sources

This work was largely supported by NIH grant HL-071797 & HL-076167 to LEO and in part by grants from the Medical Research Council G0600270 and G0601295 to AA.

We thank the Julie Henry Fund at the Transplant Center of the BIDMC for their support. We thank Dr. Shiva Gautam from the BIDMC Biostatistics Program and Harvard University Clinical and Translational Science Center for his assistance with biostatistics. LEO is a consultant of Ikaria Inc.

References

1. Cook DN, Pisetsky DS, Schwartz DA. Toll-like receptors in the pathogenesis of human disease. Nature immunology 2004;5:975–979. [PubMed: 15454920]

2. Ishikawa K, Sugawara D, Wang X, Suzuki K, Itabe H, Maruyama Y, Lusis A. J Heme oxygenase-1 inhibits atherosclerotic lesion formation in ldl-receptor knockout mice. Circ Res 2001;88:506–512. [PubMed: 11249874]

3. Libby P, Pober JS. Chronic rejection. Immunity 2001;14:387–397. [PubMed: 11336684]

4. Nobuyoshi M, Kimura T, Nosaka H, Mioka S, Ueno K, Yokoi H, Hamasaki N, Horiuchi H, Ohishi H. Restenosis after successful percutaneous transluminal coronary angioplasty: serial angiographic follow-up of 229 patients. J Am Coll Cardiol 1988;12:616–623. [PubMed: 2969925]

5. Serruys PW, Luijten HE, Beatt KJ, Geuskens R, de Feyter PJ, van den Brand M, Reiber JH, ten Katen HJ, van Es GA, Hugenholtz PG. Incidence of restenosis after successful coronary angioplasty: a time-related phenomenon. A quantitative angiographic study in 342 consecutive patients at 1, 2, 3, and 4 months. Circulation 1988;77:361–371. [PubMed: 2962786]

6. Elezi S, Kastrati A, Neumann FJ, Hadamitzky M, Dirschinger J, Schomig A. Vessel size and long-term outcome after coronary stent placement. Circulation 1998;98:1875–1880. [PubMed: 9799207]

7. Degertekin M, Serryus PW, Foley DP, Tanabe K, Regar E, Vos J, Smits PC, van der Giessen WJ, van den Braund M, de Feyer P, Popma JJ. Persistent inhibition of neointimal hyperplasia after sirolimus-eluting stent implantation. Circulation 2002;106:1610–1613. [PubMed: 12270850]

8. Morice MC, Serruys PW, Sousa JE, Fajadet J, Ban Hayashi E, Perin M, Colombo A, Schuler G, Barragan P, Guagliumi G, Molnàr F, Falotico R. RAVEL Study Group. A randomized comparison of a sirolimus-eluting stent with a standard stent for coronary revascularization. N Engl J Med 2002;346:1773–1780. [PubMed: 12050336]

9. Otterbein LE, Zuckerbraun BS, Haga M, Liu F, Song R, Usheva A, Stachulak C, Bodyak N, Smith RN, Csizmadia E, Tyagi S, Akamatsu Y, Flavell RJ, Billiar TR, Tzeng E, Bach FH, Choi AM, Soares MP. Carbon monoxide suppresses arteriosclerotic lesions associated with chronic graft rejection and with balloon injury. Nature medicine 2003;9:183–190.

10. Ryter SW, Otterbein LE. Carbon monoxide in biology and medicine. Bioessays 2004;26:270–280. [PubMed: 14988928]

11. Scott JR, Chin BY, Bilban MH, Otterbein LE. Restoring HOmeostasis: is heme oxygenase-1 ready for the clinic? Trends Pharmacol Sci 2007;28:200–205. [PubMed: 17416426]

12. Li Volti G, Sacerdoti D, Sangras B, Vanella A, Mezentsev A, Scapagnini G, Falck JR, Abraham NG. Carbon monoxide signaling in promoting angiogenesis in human microvessel endothelial cells. Antioxidants & redox signaling 2005;7:704–710. [PubMed: 15890016]

13. Brouard S, Berberat PO, Tobiasch E, Seldon MP, Bach FH, Soares MP. Heme oxygenase-1-derived carbon monoxide requires the activation of transcription factor NF-kappa B to protect endothelial cells from tumor necrosis factor-alpha-mediated apoptosis. The Journal of biological chemistry 2002;277:17950–17961. [PubMed: 11880364]

14. Lopez-Farre A, Sanchez de Miguel L, Caramelo C, Gomez-Macias J, Garcia R, Mosquera JR, de Frutos T, Millas I, Rivas F, Echezarreta G, Casado S. Am J Physiol 1997;272:760–768.

15. Ono Y, Ono H, Matsuoka H, Fujimori T, Frohlich ED. Apoptosis, coronary arterial remodeling, and myocardial infarction after nitric oxide inhibition in SHR. Hypertension 1999;34:609–616. [PubMed: 10523335]

16. Cooke JP. NO and angiogenesis. Atheroscler Suppl 2003;4:53–60. [PubMed: 14664903]

17. Schlaeger TM, Bartunkova S, Lawitts JA, Teichmann G, Risau W, Deutsch U, Sato TN. Uniform vascular-endothelial-cell-specific gene expression in both embryonic and adult transgenic mice. Proc Natl Acad Sci U S A 1997;94:3058–3063. [PubMed: 9096345]

18. Suriano R, Chaudhuri D, Johnson RS, Lambers E, Ashok BT, Kishore R, Tiwari RK. 17Beta-estradiol mobilizes bone marrow-derived endothelial progenitor cells to tumors. Cancer Res 2008;68:6038–6042. [PubMed: 18676823]

19. Chin BY, Jiang G, Wegiel B, Wang HJ, Macdonald T, Zhang XC, Gallo D, Cszimadia E, Bach FH, Lee PJ, Otterbein LE. Hypoxia-inducible factor 1alpha stabilization by carbon monoxide results in cytoprotective preconditioning. Proc Natl Acad Sci U S A 2007;104:5109–5114. [PubMed: 17360382]

20. Wiggan OSA, Bamburg JR. Essential requirement for Rho family GTPase signaling in Pax3 induced mesenchymal-epithelial transition. Cell Signal. 2006

21. Ahmed A, Dunk C, Kniss D, Wilkes M. Role of VEGF receptor-1 (Flt-1) in mediating calcium-dependent nitric oxide release and limiting DNA synthesis in human trophoblast cells. Lab Invest 1997;76:779–791. [PubMed: 9194854]
22. Fondevila C, Shen XD, Tsuchiyashi S, Yamashita K, Csizmadia E, Lassman C, Busuttil RW, Kupiec-Weglinski JW, Bach FH. Biliverdin therapy protects rat livers from ischemia and reperfusion injury. Hepatology (Baltimore, Md) 2004;40:1333–1341.
23. Gill M, Dias S, Hattori K, Rivera ML, Hicklin D, Witte L, Girardi L, Yurt R, Himel H, Rafii S. Vascular trauma induces rapid but transient mobilization of VEGFR2(+)AC133(+) endothelial precursor cells. Circ Res 2001;88:167–174. [PubMed: 11157668]
24. Song R, Mahidhara RS, Liu F, Ning W, Otterbein LE, Choi AM. Carbon monoxide inhibits human airway smooth muscle cell proliferation via mitogen-activated protein kinase pathway. American journal of respiratory cell and molecular biology 2002;27:603–610. [PubMed: 12397020]
25. Peyton KJ, Reyna SV, Chapman GB, Ensenat D, Liu XM, Wang H, Schafer AI, Durante W. Heme oxygenase-1-derived carbon monoxide is an autocrine inhibitor of vascular smooth muscle cell growth. Blood 2002;99:4443–4448. [PubMed: 12036874]
26. Basile JR, Gavard J, Gutkind JS. Plexin-B1 utilizes RhoA and Rho kinase to promote the integrin-dependent activation of Akt and ERK and endothelial cell motility. J Biol Chem 2007;282:34888–34895. [PubMed: 17855350]
27. Zhang X, Shan P, Alam J, Fu XY, Lee PJ. Carbon monoxide differentially modulates STAT1 and STAT3 and inhibits apoptosis via a phosphatidylinositol 3-kinase/Akt and p38 kinase-dependent STAT3 pathway during anoxia-reoxygenation injury. J Biol Chem 2005;280:8714–8721. [PubMed: 15590660]
28. Fujimoto H, Ohno M, Ayabe S, Kobayashi H, Ishizaka N, Kimura H, Yoshida K, Nagai R. Carbon monoxide protects against cardiac ischemia--reperfusion injury in vivo via MAPK and Akt--eNOS pathways. Arteriosclerosis, thrombosis, and vascular biology 2004;24:1848–1853.
29. Song R, Mahidhara RS, Liu F, Ning W, Otterbein LE, Choi AM. Carbon monoxide inhibits human airway smooth muscle cell proliferation via mitogen-activated protein kinase pathway. Am J Respir Cell Mol Biol 2002;27:603–610. [PubMed: 12397020]
30. Batzlsperger CA, Achatz S, Spreng J, Riegger GA, Griese DP. Evidence for a possible inhibitory interaction between the HO-1/CO- and Akt/NO-pathways in human endothelial cells. Cardiovasc Drugs Ther 2007;21:347–355. [PubMed: 17896171]
31. Zuckerbraun BS, Billiar TR, Otterbein SL, Kim PK, Liu F, Choi AM, Bach FH, Otterbein LE. Carbon monoxide protects against liver failure through nitric oxide-induced heme oxygenase 1. The Journal of experimental medicine 2003;198:1707–1716. [PubMed: 14657222]
32. Zuckerbraun BS, Chin BY, Wegiel B, Billiar TR, Czsimadia E, Rao J, Shimoda L, Ifedigbo E, Kanno S, Otterbein LE. Carbon monoxide reverses established pulmonary hypertension. J Exp Med 2006;203:2109–2119. [PubMed: 16908624]
33. Zuckerbraun BS, Billiar TR, Otterbein SL, Kim PK, Liu F, Choi AM, Bach FH, Otterbein LE. J Exp Med 2003;198:1707–1716. [PubMed: 14657222]
34. Ziche M, Morbidelli L, Masini E, Granger H, Geppetti P, Ledda F. Nitric oxide promotes DNA synthesis and cyclic GMP formation in endothelial cells from postcapillary venules. Biochem Biophys Res Commun 1993;192:1198–1203. [PubMed: 8389543]
35. Dimmeler S, Fleming I, Fisslthaler B, Hermann C, Busse R, Zeiher AM. Activation of nitric oxide synthase in endothelial cells by Akt-dependent phosphorylation. Nature 1999;399:601–605. [PubMed: 10376603]
36. Dimmeler S, Zeiher AM. Nitric oxide-an endothelial cell survival factor. Cell Death Differ 1999;6:964–968. [PubMed: 10556973]
37. Tanner FC, Meier P, Greutert H, Champion C, Nabel EG, Luscher TF. Nitric oxide modulates expression of cell cycle regulatory proteins: a cytostatic strategy for inhibition of human vascular smooth muscle cell proliferation. Circulation 2000;101:1982–1989. [PubMed: 10779466]
38. Ceneviva GD, Tzeng E, Hoyt DG, Yee E, Gallagher A, Engelhardt JF, Kim YM, Billiar TR, Watkins SA, Pitt BR. Nitric oxide inhibits lipopolysaccharide-induced apoptosis in pulmonary artery endothelial cells. Am J Physiol 1998;275:717–728.

39. Williams SE, Wootton P, Mason HS, Bould J, Iles DE, Riccardi D, Peers C, Kemp PJ. Hemoxygenase-2 is an oxygen sensor for a calcium-sensitive potassium channel. Science 2004;306:2093–2097. [PubMed: 15528406]
40. Deshane J, Chen S, Caballero S, Grochot-Przeczek A, Was H, Li Calzi S, Lach R, Hock TD, Chen B, Hill-Kapturczak N, Siegal GP, Dulak J, Jozkowicz A, Grant MB, Agarwal A. Stromal cell-derived factor 1 promotes angiogenesis via a heme oxygenase 1-dependent mechanism. J Exp Med 2007;204:605–618. [PubMed: 17339405]
41. Aicher A, Heeschen C, Mildner-Rihm C, Urbich C, Ihling C, Technau-Ihling K, Zeiher AM, Dimmeler S. Nat Med 2003;9:1370–1376. [PubMed: 14556003]
42. Morishita R, Gibbons GH, Horiuchi M, Ellison KE, Nakajima M, Zhang L, Kaneda Y, Ogihara T, Dzau VJ. Proc Natl Acad Sci USA 1995;92:5855–5859. [PubMed: 7597041]
43. Morishita R, Gibbons GH, Ellison KE, Nakajima M, Zhang L, Kaneda Y, Ogihara T, Dzau VJ. Single intraluminal delivery of antisense cdc2 kinase and proliferating-cell nuclear antigen oligonucleotides results in chronic inhibition of neointimal hyperplasia. Proc Natl Acad Sci U S A 1993;90:8474–8478. [PubMed: 8104336]
44. Luo Y, Marx SO, Kiyokawa H, Koff A, Massague J, Marks A. Rapamycin resistance tied to defective regulation of p27kip1. Mol Cell Biol 1996;16:6744–6751. [PubMed: 8943329]
45. Gomes D, Louedec L, Plissonnier D, Dauge MC, Henin D, Osborne-Pellegrin M, Michel JB. Endoluminal smooth muscle cell seeding limits intimal hyperplasia. J Vasc Surg 2001;34:707–715. [PubMed: 11668328]

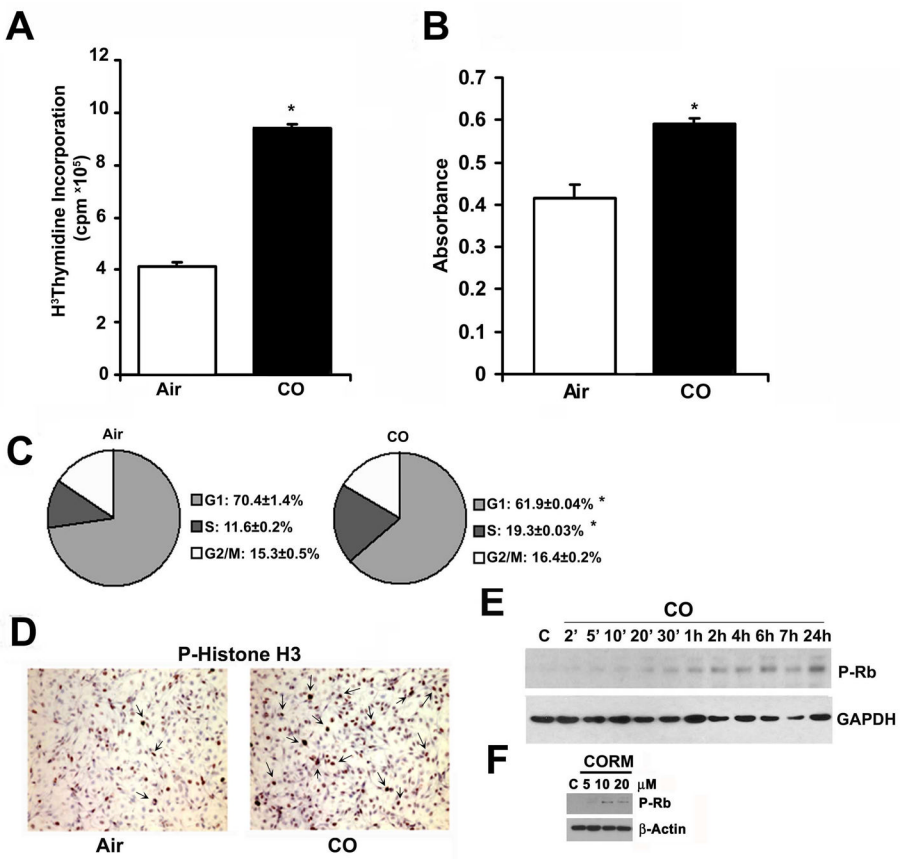

Figure 1. Carbon monoxide controls cell cycle progression and induces proliferation of RAEC cells

A. ^{3}H-thymidine incorporation into DNA was used to assess proliferation ± CO. Results represent mean ± SD of three independent experiments (n=6/group). One-way ANOVA; *p<0.05 vs air-treated. **B.** BrdU incorporation to assess proliferation of air and CO-treated RAEC cells measured at 24 hours. Results represent mean ± SD of six independent experiments with n=3/group. One-way ANOVA; *p<0.018 CO vs Air. **C.** Cell cycle analysis of cells treated ± CO for 10 hours. Results represent mean ± SD of three independent experiments with n=3/group. One-way ANOVA; *p<0.008 S-phase, *p=0.04 G1, CO vs Air. **D**. Phospho-histone H3 immunostaining of cells exposed to air or CO for 24 hr. Representative images from 10–15 fields from 2 independent experiments are shown. Arrows indicate positive stained mitotic bodies. **E.** P-Rb immunoblotting in cells treated ± CO for the indicated time points. Blot is representative of 2 independent experiments. **F**. P-Rb immunoblot in cells treated ± CORM ALF 421 (5–20μM) for 24 hours. Blot is representative of 3 independent experiments.

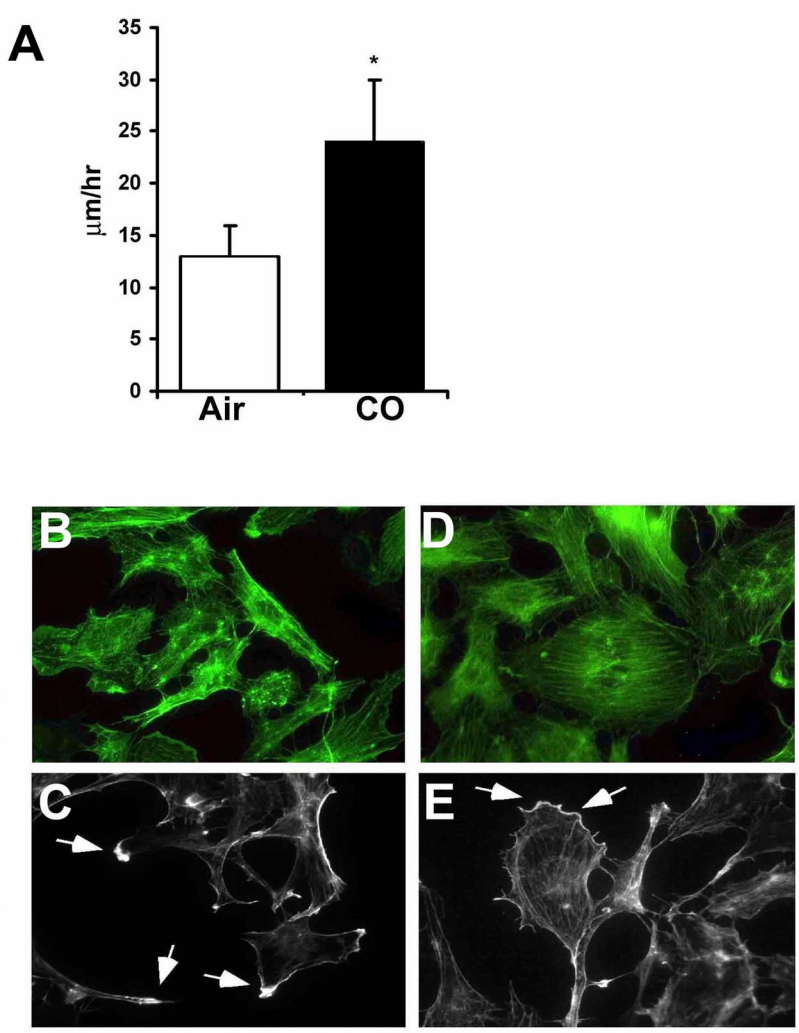

Figure 2. Carbon monoxide enhances motility and modulates cytoskeletal changes in RAEC

A. Bar graph of the average speeds of RAEC along ± CO. Data are representative of 3 independent experiments. Results represent the mean distance traveled ± SD of 120 cells in each treatment group counted in three independent experiments. Five separate fields were monitored over the course of 24–48 hr with images taken of each field every 5 minutes. Values from 5 fields of CO and air treated cells were used to calculate mean± SD; One-way ANOVA; *$p<0.02$. Note that CO more then doubled the speed of cell migration following insult. **B–E.** Phalloidin staining of cells treated with air (**A–B**) or CO (**D–E**) for 24h. Arrows indicates the accumulation of F-actin at the leading edge of cells indicative of directed growth. Images are representative of 2 independent experiments from 6–10 images/slide in each treatment group.

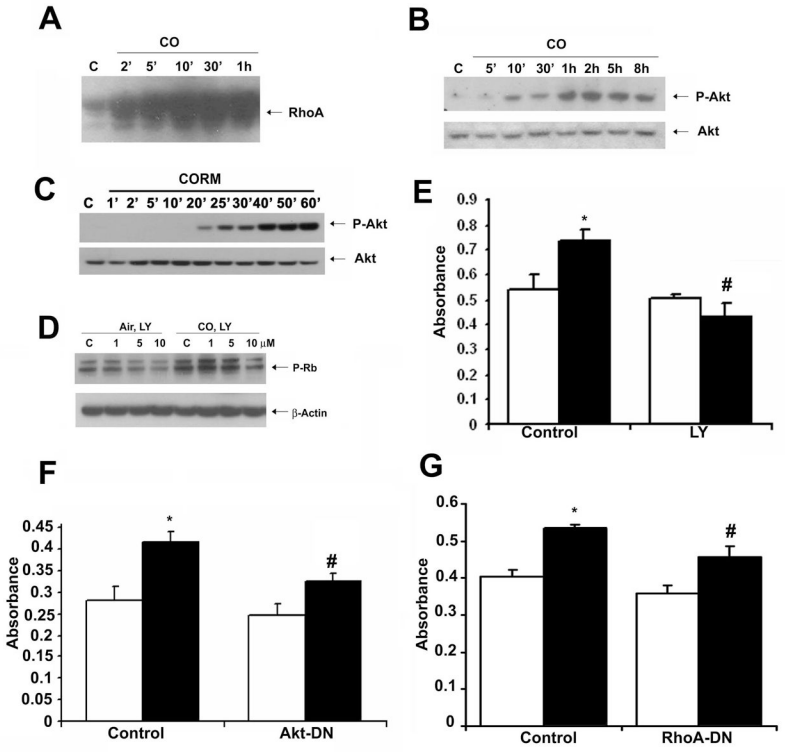

Figure 3. Carbon monoxide activates RhoA-PI3K-Akt signaling pathway to induce proliferation of RAEC cells

A. Activity of small GTPase, RhoA was tested using the Rhotekin-RBD fused with GST to precipitate GTP-RhoA in cells treated with CO for the indicated times. **B**. P-Akt immunoblot **in** cells exposed to CO for 5min-8 h. Membranes were reprobed for total Akt as loading control. **C.** P-Akt immunoblot in cells treated ± CORM ALF 421 (20 μM in dH_2O) for 1–60 minutes. **D.** RAEC were pretreated with LY290024 inhibitor (1–10 mM) for 1hr followed by exposure to air or CO for 6 hr. P-Rb was measured by immunoblotting. Controls were treated with DMSO alone. **E**. Proliferation in cells pretreated with LY290034 inhibitor (10 mM) followed by exposure to air (open bars) or CO (solid bars) for 24 hr. Proliferation was measured by BrdU incorporation. Results represent mean ± SD of three independent experiments with n=3/group. Two-way ANOVA was applied to compare between groups; p=0.002. Tukey post-hoc test showed *CO vs Air; #p=0.005 #CO+LY vs CO; p<0.001. **F**. BrdU incorporation of RAEC transiently transfected with DN-Akt or empty vector as control and exposed to air (open bars) or CO (solid bars). Data represent mean ± SD of four independent experiments n=3/group, Two-way ANOVA, p<0.0001. Tukey post-hoc; *p<0.0001 CO vs Air; #p<0.0001 CO+DN-Akt vs CO+empty vector. Transfection efficiency was determined to be 40–50% by transfection with a GFP expression vector. **G**. BrdU incorporation in RAEC were infected with Ad-RhoA-DN or Ad-LacZ as control for 48 hr in the presence of air (open bars) or CO (solid bars) for 24 hr. Data represent mean ± SD of four independent experiments with n=3/treatment group. CO vs Air and CO+Ad-RhoA vs CO+Ad-LacZ; Two-way ANOVA, p<0.0001; Tukey post-hoc *p<0.0001 CO vs Air; #p<0.0001 CO+Ad-RhoA vs CO+Ad-LacZ. All immunoblots presented are representative of 2–3 independent experiments.

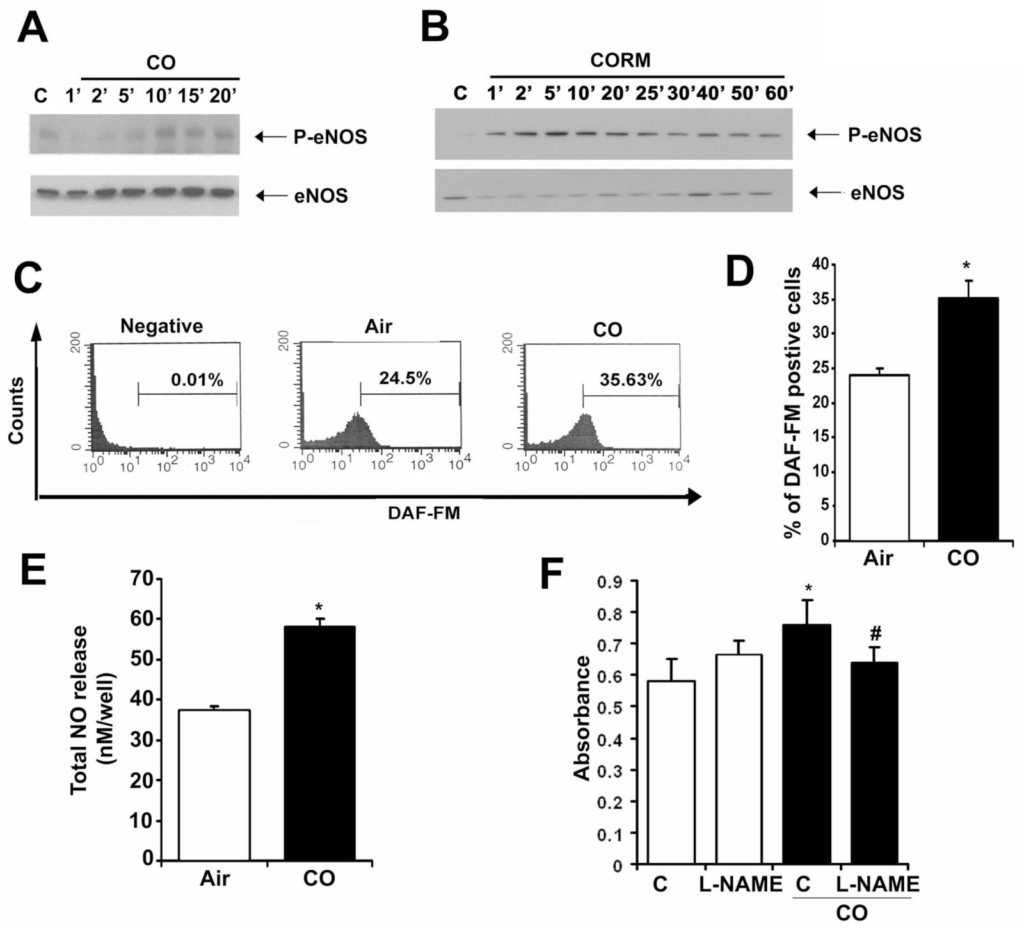

Figure 4. Nitric oxide mediates the proliferative enhancing effects of CO in RAEC

A. Phospho-eNOS immunoblot of CO-exposed RAEC. Membranes were reprobed for total eNOS as loading control. RAEC cells were treated with 250 ppm CO for the indicated time points. **B.** Phospho-eNOS immunoblotting in RAEC treated ± CORM ALF 421 (20 μM) for the indicated time points. **C–D.** Nitric oxide production in RAEC ± CO for 5′ and measured by FACS using DAF-FM. Representative analyses (**C**) and quantitation (**D**) are shown. Data represent mean ± SD from four independent experiments with n=3/group; Wilcoxon non-parametric test; *p=0.05 CO vs air. **E**. Total nitric oxide production was measured in the media of HUVEC cells stimulated with CO for 1 hr. Data represent mean ± SD from three independent experiments with n=3–6/group; One way-ANOVA; *p<0.0001 CO vs air. **F.** BrdU incorporation in RAEC pre-treated for 1 hour with 100 mM L-NAME or dH_20 as vehicle control followed by treatment with air or CO as above. Data represent mean ± SD from three independent experiments with n=3/group; Two-way ANOVA, p=0.002. Tukey post-hoc; *p<0.001 CO vs Air; #p<0.001 CO+L-NAME versus CO. All immunoblots are representative of 3 independent experiments.

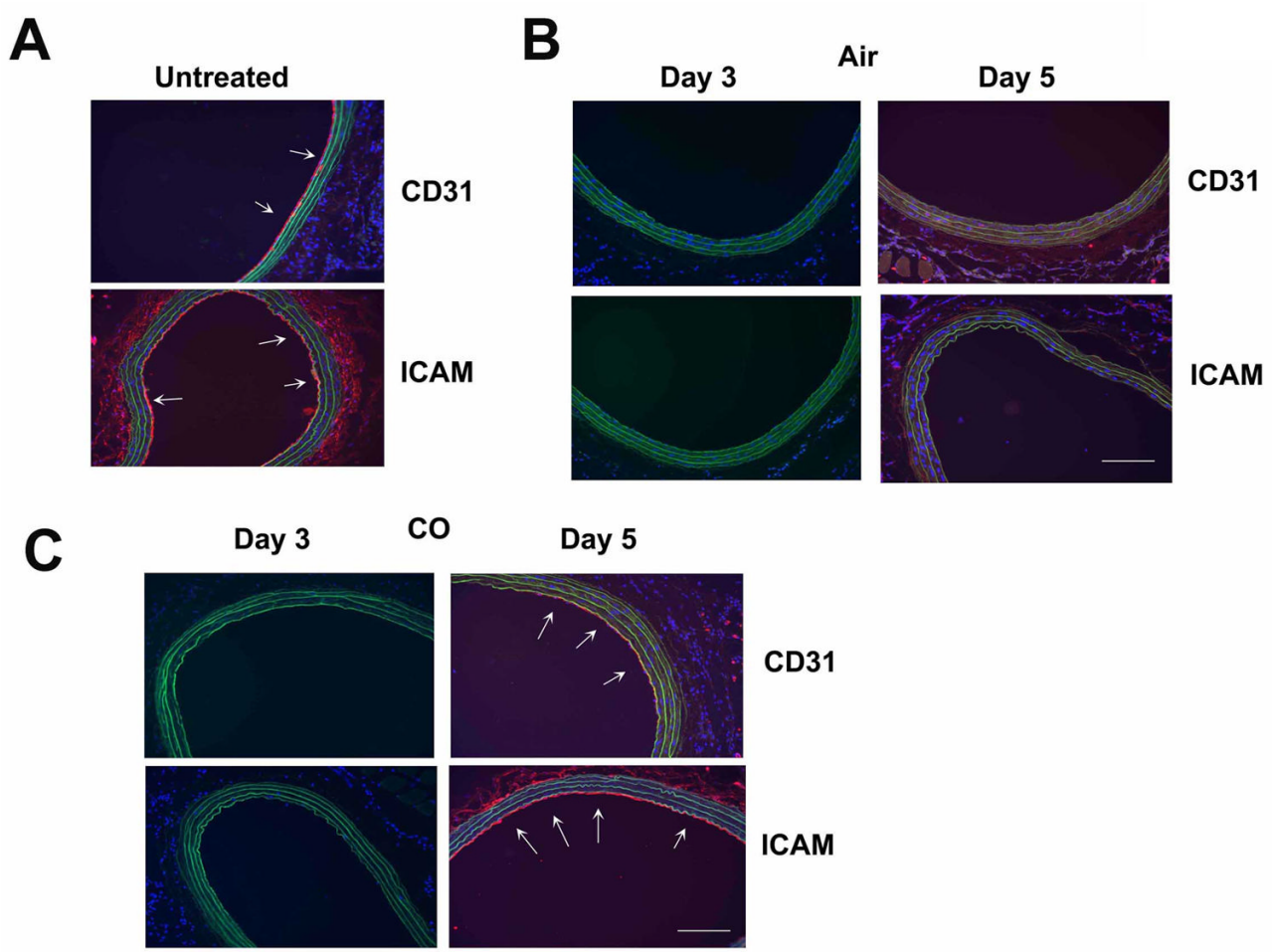

Figure 5. Carbon monoxide induces reendothelialization following balloon injury in rats

A–C. Immunostaining for CD31 and ICAM in non-injured rat carotids at 3 and 5 days after balloon injury in animals pretreated with Air (**B**) or CO (**C**). CO was administered for 1 hr at 250 ppm. Images are representative of 6–8 images from each vessel isolated from 4–6 rats/ treatment group. Note that CO-treated rats have CD31 and ICAM positive staining at day 5, which was not present in air-treated animals.

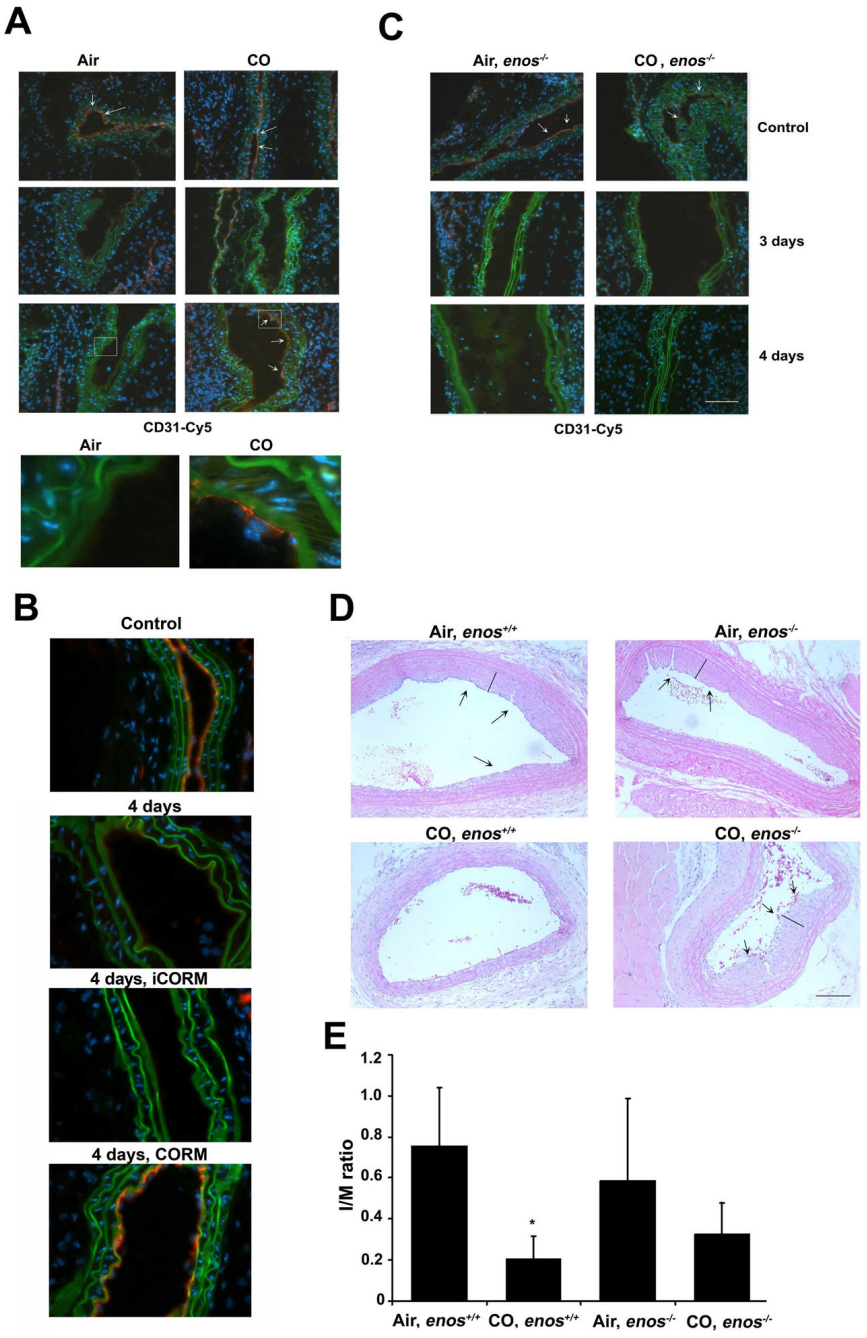

Figure 6. Carbon monoxide enhances re-endothelialization after wire injury in mice that is dependent on eNOS

A–B. Immunostaining for CD31, 3 and 4 days after wire injury of carotid arteries in mice exposed to Air or CO as described. Images were taken under magnification of 20× (upper figure; scale bar=50 μm) and 63× (inset below). **B**. Immunostaining for CD31 in injured mice treated with CORM ALF421 or iCORM 10 mg/kg, i.p. as described in Materials and Methods. Control-naive vessel, 4 days injured untreated, 4 days injured + iCORM, 4days injured + CORM ALF421. **C**. *enos*$^{-/-}$ mice were treated with air or CO 1 hr prior to injury. Injured vessels were harvested at day 4. All images are representative of 8–10 fields at 40× magnification and are representative of 4–6 mice/group. **D.** H&E staining of control and injured

vessels 2 weeks after injury from wt and *enos*$^{-/-}$ mice pretreated with air or CO. Images are representative of 4–6 fields from 3–5 mice/group. 20× magnification, scale bar =50 μm. Black line indicates the neo-intima. **E.** Quantitation of intimal expansion expressed as I:M ratio from n=4–6 mice/group. 2-way ANOVA p=0.02; Tukey post-hoc Air +*enos*$^{+/+}$ and CO+*enos*$^{+/+}$ groups; *p=0.025 and CO+*enos*$^{-/-}$ vs Air+ *enos*$^{-/-}$; p=0.364.

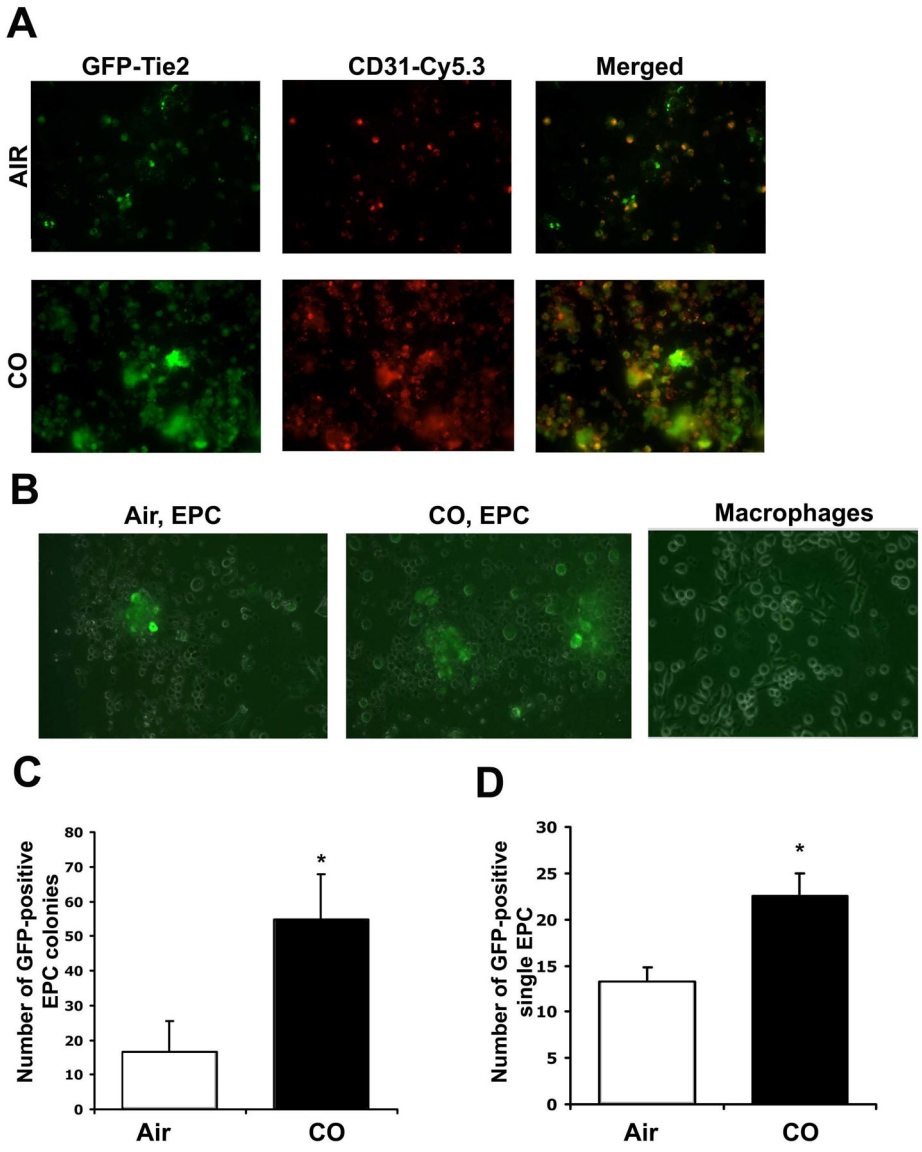

Figure 7. Carbon monoxide augments endothelial progenitor cell expansion in vitro

A. Immunostaining for CD31 (red) and GFP (green) positive staining of bone marrow derived EPC isolated from Tie2-GFP mice treated ± CO for 72 hr in the presence of EC growth factors. Images are representative of 4–6 fields from 2 independent experiments of n=6/group. Note that CO enhanced EC differentiation. **B**. Expansion of EPC by CO is specific. Bone marrow from Tie-2-FGP mice was differentiated into either EC (left and center panels) or macrophages (right panel). CO enhanced GFP expression and therefore Tie-2 expression in EC differentiated, but not macrophage-differentiated populations. Representative Tie-2 GFP positive EPC and Tie2-GFP negative macrophage colonies are shown. Images are representative of 4–6 fields from 2 independent experiments of n=3/group. **C–D**. Quantitation of colonies (**C**) and single (**D**) GFP-positive cells. Results represent mean ± SD of three independent experiments with n=4–5/group; 1-way ANOVA *p<0.0001 CO vs Air in C and *p=0.001 in D. Note that CO enhanced both the number of colonies and single cell populations. Scale bar=50μm.

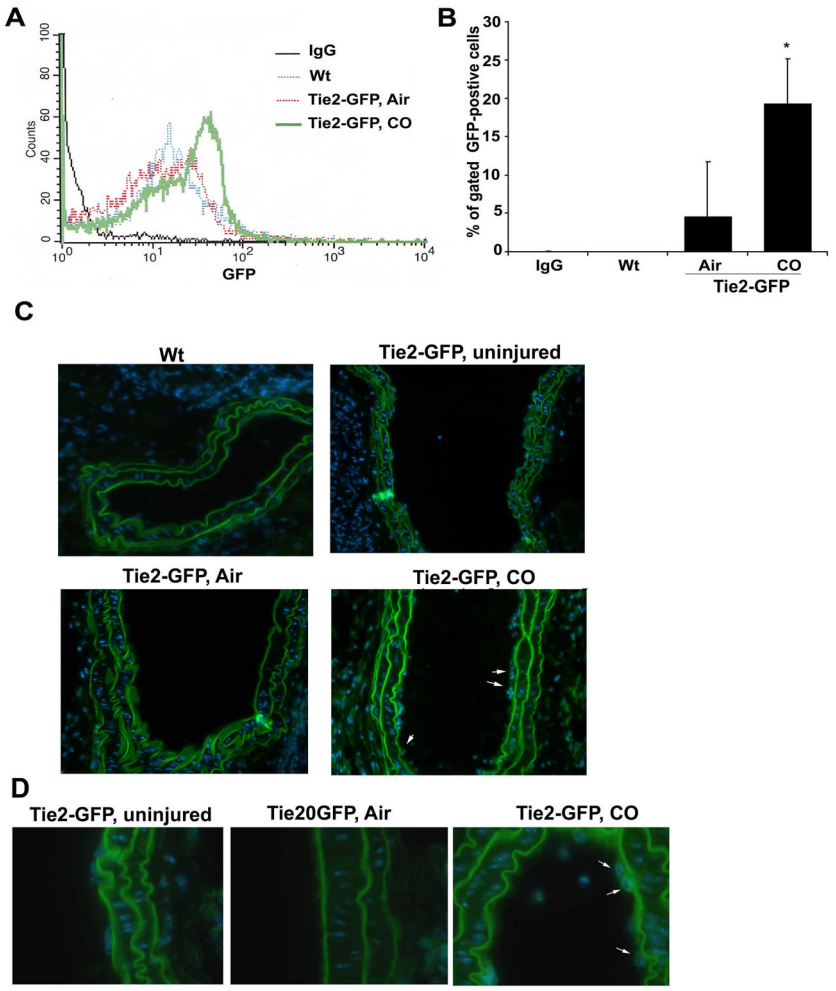

Figure 8. CO induces GFP-positive EPC peripheral mobilization and recruitment to injured vessels in mice

A. Representative flow cytometric analysis of GFP-positive cells in peripheral blood from Tie-2 GFP chimeric mice 12 hrs after wire trauma. Isotype control (IgG), Wt-injured, Air/Tie-2-GFP-injured and CO/Tie-2-GFP-injured samples are shown. **B.** Quantitation of GFP-positive cells in peripheral blood. Data represent mean ± SD (n=3 mice/group). Non-parametric Wilcoxon test; *p=0.05 CO vs Air. **C–D.** Immunofluorescent staining for GFP-Tie2-positive endothelial cells in the vessels 4 days after wire-injury performed in Tie-2-GFP chimeric mice. Representative images of GFP fluorescence in wt (non-Tie2-GFP, Tie2-GFP uninjured, GFP-Tie2 chimeric mice treated with CO (250 ppm or 1 hr prior to injury) or Air. Representative images of 8–10 sections from n=2–4 vessel regions/mouse/group; n=4–6 mice/treatment group. Magnification is 20× (**C**) and 63× (**D**). Scale bar=50μm. Arrows indicate GFP positive cells. Note that elastin fibers in the media autofluoresce at these wavelengths.